# Nonlinear dynamics of a Heisenberg ferromagnet

R. S. Fishman
*Department of Physics, SU Station Box 5566, North Dakota State University, Fargo, North Dakota 58105-5566* and Solid State Division, P. O. Box 2008, Oak Ridge National Laboratory, Oak Ridge, Tennessee 37831*

S. H. Liu
*Solid State Division, P. O. Box 2008, Oak Ridge National Laboratory, Oak Ridge, Tennessee 37831*
(Received 21 May 1991)

Using an expansion technique we study the dynamics of a spin-$s$ Heisenberg ferromagnet with nearest-neighbor exchange coupling $J$. The transverse-mode frequencies are calculated by expanding a self-energy function in powers of $1/z$, where $z$ is the number of nearest neighbors on the lattice. To zeroth-order in $1/z$, the mode frequencies agree with the random-phase approximation. To the next order in $1/z$, the coupling between the transverse and longitudinal fluctuations is responsible for a shift in the spin-wave (SW) frequencies $\omega_{\mathbf{k}}$ and for the appearance of a second pole in the correlation function at an energy close to $zJs$. This second mode is excited by longitudinal fluctuations, which force the local spin to precess about the mean field with frequency $zJs$ rather than with the spin-wave frequency $\omega_{\mathbf{k}}$. Because of its interactions with the surrounding spins, this precession can propagate through the lattice. When $\omega_{\mathbf{k}}$ is close to $zJs$, the precessional mode may be observable as a splitting of the transverse resonance into two peaks. Since the coupling between the longitudinal and transverse fluctuations becomes exponentially small at low temperatures, the precessional mode only appears above the crossover temperature $\bar{T}\approx 0.2zJs$. Because the SW approximation mishandles the subtle interplay between the longitudinal and transverse fluctuations, it misses the second pole in the correlation function. In agreement with earlier work we find that the SW approximation breaks down above the temperature $\bar{T}$, when the exponential coupling terms in the correlation function become significant. Although the precessional mode is induced by longitudinal fluctuations, it is fundamentally a transverse excitation and must be distinguished from the longitudinal mode, which has zero frequency.

## I. INTRODUCTION

At low temperatures, the spin-wave (SW) approximation has been remarkably successful[1] in predicting the thermodynamic and dynamic properties of a ferromagnet. But even Dyson,[2] who pioneered the SW approximation, recognized that its basic assumptions must break down when the temperature becomes sufficiently high. At high temperatures, the interactions between spin waves become highly nonlinear and the concept of a weakly interacting transverse excitation loses its meaning. The consequences of this breakdown have gone largely unstudied, mostly because the observed SW frequencies[3,4] of a ferromagnet remain quite close to the predictions of the SW approximation even near the Curie temperature $T_C$. In a previous paper,[5] Fishman and Vignale (FV) used a rigorous expansion of the free energy to predict that the SW approximation would fail above the crossover temperature $\bar{T}\approx 0.2zJs$, where $z$ is the coordination number of the lattice, $s$ is the spin, and $J$ is the ferromagnetic coupling constant. This thermodynamic crossover is marked by a peak in the fluctuation specific heat.[6] In this paper, we examine the consequences of the breakdown of the SW approximation for the dynamics of a ferromagnet.

Using an expansion of the correlation function, we find that the mode frequencies deviate from the SW predictions above a temperature very close to $\bar{T}$. Hence, the thermodynamic and dynamic crossover temperatures agree. Above $\bar{T}$, the modes can no longer be described as weakly interacting, particlelike excitations. As discussed in FV, the many-body interactions between the spin waves contribute to the free energy above $\bar{T}$. In this paper, we find that the coupling between the transverse and longitudinal fluctuations also becomes significant above $\bar{T}$ and shifts the SW frequencies.

Much more surprisingly, the longitudinal fluctuations are responsible for a second pole in the transverse correlation function near the energy $\Delta\approx zJs$. At this energy, a longitudinal fluctuation forces the spin to precess about the local mean field with frequency $\Delta$. Due to its coupling with the surrounding spins, the precessional mode can propagate through the lattice. The precessional mode is absent in the SW approximation, which mishandles the subtle interplay between the longitudinal and transverse degrees of freedom.

Because they are strongly coupled and highly nonlinear, the "spin-wave" modes above $\bar{T}$ are quite different from the linear excitations below $\bar{T}$. But, to avoid confusion, we continue to refer to these excitations, both above and below the crossover temperature, as spin-wave modes. When the SW frequency $\omega_{\mathbf{k}}$ is close to $\Delta$, the mixing between the SW and precessional modes splits the transverse resonance into two peaks. Due to this mixing,

 

there is really no sharp distinction between the SW and precessional branches of transverse excitations.

In earlier work, FV studied the breakdown of the SW approximation by expanding the SW and exact free energies in powers of $1/z$. To zeroth and first order in $1/z$, the SW free energy is exact. But to order $1/z^2$, the SW free energy deviates from the exact free energy above the crossover temperature $\overline{T}$, which is marked by a peak in the fluctuation specific heat.[5,6] Since the Curie temperature scales like $zJs^2$, the nonlinear regime between $\overline{T} \propto zJs$ and $T_C$ grows with increasing spin. Above $\overline{T}$, the exponentially small terms in the free energy become important and the asymptotic, low-temperature expansion of the free energy breaks down. Hence, the failure of the SW approximation follows the pattern predicted by Dyson.[2]

In this paper, we use a related technique to evaluate the mode frequencies of a ferromagnet. Instead of expanding the free energy, we expand a self-energy function $\Sigma(\mathbf{k},i\omega_m)$ which is proportional to the inverse of the transverse correlation function $D_{+-}(\mathbf{k},i\omega_m)$. If $\Sigma(\mathbf{k},i\omega_m)$ is expanded to zeroth-order in $1/z$, the correlation function has poles at the SW frequencies of the random-phase approximation[1] (RPA). If $\Sigma(\mathbf{k},i\omega_m)$ is expanded to order $1/z$, the SW frequencies are shifted from the result of the SW approximation and the correlation function develops a second pole near the energy $\Delta$. Both the shift in the SW frequencies and the residue of the second pole become significant only above $\overline{T}$.

The self-energy expansion technique used in this paper does not alter the spin commutation relations or simplify the spin dynamics. In the high-temperature regime above $\overline{T}$, the results of this expansion are formally exact and physically meaningful. To establish the self-consistency of this technique and to apply it to a more straightforward problem, we have studied the onset of long-range order in a paramagnet. In the preceding paper,[7] we use the self-energy expansion to show that the long-range correlations of a paramagnet diverge at the same Curie temperature previously evaluated by Fishman and Liu[6] (FL) in the ferromagnet. Hence, the self-energy expansion is consistent with the order-parameter expansion used in FL. Both the preceeding paper and the present one use the same basic methodology. First, the real-space correlation function is expanded to the required order in $1/z$. Then the real-space self-energy is obtained by inverting a matrix equation. Finally, a Fourier transformation yields $\Sigma(\mathbf{k},i\omega_m)$. All these manipulations are performed for the Matsubara correlation function and self-energy. The analytic continuation to real frequencies is left till last.

Unfortunately, the lifetime of the SW and precessional modes cannot be obtained with this approach. While the shifts in the transverse mode frequencies are analytic functions of $1/z$, the width $\Gamma$ of the modes is not. Hence, a $1/z$ expansion of $\Gamma$ always yields a vanishing result. To compensate for this weakness of the theory, we have estimated $\Gamma$ and its effect on the observability of the precessional mode.

The expansion technique used in this paper is related to the earlier work of Vaks, Larkin, and Pikin.[8] Like the present authors, Vaks *et al.* do not simplify the commutation relations of the spin operators. They evaluate the correlation function by expanding in powers of $1/r_0^3$, where $r_0$ is the range of the exchange interaction. After comparing our results with the results of Vaks *et al.*, we conclude that the $1/r_0^3$ expansion is exact to order $1/z$. As argued in Sec. V, however, the $1/r_0^3$ expansion is not exact to higher order in $1/z$. Nonetheless, the results of Vaks *et al.* provide a useful check on the $1/z$ results of this paper. Because they include terms of arbitrarily high order in $1/z$, Vaks *et al.* did not notice that the transverse correlation function develops an additional pole near $\Delta$.

To clarify the physical interpretation of the transverse pole at $\Delta$, we have also evaluated the longitudinal correlation function. After expanding to order $1/z$, we find that the longitudinal correlation function has a pole only at zero frequency. The dynamics of the longitudinal fluctuations are caused by the coupling between the longitudinal and transverse degrees of freedom. At low temperatures, when this coupling is surpressed, the longitudinal correlation function is static. Hence, we must carefully distinguish between the precessional mode with energy $\Delta$ and the longitudinal mode with zero energy.

Although fundamentally a transverse excitation, the precessional mode is excited by longitudinal fluctuations. A longitudinal fluctuation forces the local spin to precess around the mean field with frequency $\Delta$ rather than with the SW frequency $\omega_{\mathbf{k}}$. Because of its coupling with the surrounding sites, this fluctuation propagates through the lattice with an energy which depends on momentum. The propagation of the spin waves is also affected by the local, longitudinal fluctuation of a spin. Because the wave function of the spin wave contains a sum over all spin states, the spin wave can propagate through the longitudinal fluctuation with some change in energy. When $\omega_{\mathbf{k}}$ is close to $\Delta$, however, the spin waves couple strongly to the precessional mode, leading to a repulsion of the two transverse branches and a mixing of the two modes.

In the long-wavelength limit, a spin precession cannot propagate through the lattice and the residue of the pole at $\Delta$ tends to zero. So, as $\mathbf{k}\rightarrow\mathbf{0}$, the spin waves become the only transverse modes of the lattice. But, for finite wave vector, the precessional mode propagates through the lattice with a frequency shifted from $\Delta$ by dispersive effects. Although the precessional mode exists for all nonzero momentum, it is most easily observed when $\omega_{\mathbf{k}} \approx \Delta$ and when each transverse branch contains a mixture of the two modes. Away from this mode-crossing point, the residue of the pole near $\Delta$ is very small.

This paper is divided into seven sections. In Sec. II, we develop the formalism of the self-energy expansion. Applying this technique to the transverse correlation function, we evaluate the frequencies of the SW and precessional modes in Sec. III. In Sec. IV, we discuss the physical origins of the precessional mode and we demonstrate that the SW frequency deviates from the predictions of the SW approximation above the crossover temperature $\overline{T}$. In Sec. V, we estimate the width of the transverse modes and we discuss the observability of the precessional mode. Section VI is devoted to a calculation of the

longitudinal correlation function. Finally, Sec. VII contains a conclusion and discussion. In the Appendix, we prove a theorem which allows us to easily evaluate the correlation diagrams of Sec. III while retaining the full commutation relations. This theorem replaces Wick's theorem, which is not valid for spin operators.

## II. FORMALISM

In this section, we develop the self-energy expansion for a spin-$s$ Heisenberg ferromagnet with the Hamiltonian

$$H=-J\sum_{\langle i,j\rangle}\mathbf{S}_i\cdot\mathbf{S}_j\ , \tag{1}$$

where $J>0$ is the ferromagnetic coupling constant between neighboring sites. The spin operators on the $N$ lattice sites obey the commutation relations

$$[S_{\alpha i},S_{\beta j}]=-i\delta_{ij}\varepsilon_{\alpha\beta\gamma}S_{i\gamma} \tag{2}$$

with $\hbar=1$. To develop a systematic expansion for the correlation function and mode frequencies, we split the Hamiltonian into a mean-field (MF) part $H_{\rm eff}$, a constant term $H_1$, and a fluctuation term $H_2$:

$$H=H_{\rm eff}+H_1+H_2\ , \tag{3}$$

$$H_{\rm eff}=-zJM_0\sum_i S_{iz}\ , \tag{4}$$

$$H_1=\tfrac{1}{2}NzJM_0^2\ , \tag{5}$$

$$H_2=-J\sum_{\langle i,j\rangle}R_{ij}\ , \tag{6}$$

$$R_{ij}=\tilde{S}_{iz}\tilde{S}_{jz}+\tfrac{1}{2}(S_i^+S_j^-+S_i^-S_j^+)\ , \tag{7}$$

where $S_i^{\pm}=S_{ix}\pm iS_{iy}$, $\tilde{S}_{iz}=S_{iz}-M_0$ is the longitudinal fluctuation on site $i$, and $M_0$ is the mean-field order parameter $M_0=\langle S_{1z}\rangle_{\rm MF}$.

All MF expectation values are evaluated by setting $H_2$ equal to zero. Hence, the MF expectation value of the operator $A$ is given by

$$\langle A\rangle_{\rm MF}=\frac{1}{Z_0}{\rm Tr}\{e^{-\beta H_{\rm eff}}A\}\ , \tag{8}$$

$$Z_0={\rm Tr}\{e^{-\beta H_{\rm eff}}\}\ . \tag{9}$$

Because $H_1$ is a constant, it does not contribute to the MF expectation value. Every MF expectation value is a function only of the dimensionless temperature $T^*=T/zJ$ and the spin $s$.

Because the MF expectation value of $H_2$ vanishes, $H_2$ is the energy produced by the coupling of fluctuations on neighboring lattice sites. As the number of nearest neighbors $z$ increases, the mean field $zJM_0$ experienced by each spin becomes stronger and the coupling of fluctuations becomes weaker. In the limit $z\rightarrow\infty$, MF theory becomes exact and $H_2$ can be neglected. So the effects of $H_2$ can be studied with a $1/z$ expansion about MF theory.

Since $H_{\rm eff}$ commutes with $H_2$, the exact expectation value of $A$ is given by

$$\langle A\rangle=\frac{1}{Z}{\rm Tr}\{e^{-\beta H_{\rm eff}}e^{-\beta H_2}A\}\ , \tag{10}$$

$$Z={\rm Tr}\{e^{-\beta H_{\rm eff}}e^{-\beta H_2}\}\ . \tag{11}$$

The $1/z$ expansion of $\langle A\rangle$ is generated by first expanding the exponents $e^{-\beta H_2}$ in Eqs. (10) and (11), and then collecting all the terms of a given order in $1/z$:

$$\langle A\rangle=A_0(T^*)+\frac{1}{z}A_1(T^*)+\cdots\ . \tag{12}$$

The zeroth-order term $A_0$ is just the MF expectation value $\langle A\rangle_{\rm MF}$. If $A$ is dimensionless, then each coefficient $A_n$ is a function only of $T^*$ and $s$. The higher-order coefficients $A_{n\geq 1}$ are produced by the coupling of fluctuations on neighboring lattice sites.

Examples of this procedure are contained in FL and FV. In FL, we found that the coupling of fluctuations suppresses the order parameter from its MF value. By setting the total order parameter to zero, we obtained a $1/z$ expansion of the Curie temperature $T_C$. In FV, the free energy $F/NzJ$ was expanded to second order in $1/z$. The second-order free energy $F_2/NzJ$ depends not only on $T^*$ and $s$ but also on the lattice topology.

The goal of this paper is to evaluate the transverse and longitudinal correlation functions

$$D_{+-}(\mathbf{k},i\omega_m)=\sum_i e^{-i\mathbf{k}\cdot\mathbf{R}_i}D_{1i}^{+-}(i\omega_m)\ , \tag{13}$$

$$D_{ij}^{+-}(i\omega_m)=-\int_0^\beta d\tau\, e^{i\omega_m\tau}\langle T_\tau S_i^+(\tau)S_j^-(0)\rangle\ , \tag{14}$$

$$D_{zz}(\mathbf{k},i\omega_m)=\sum_i e^{-i\mathbf{k}\cdot\mathbf{R}_i}D_{1i}^{zz}(i\omega_m)\ , \tag{15}$$

$$D_{ij}^{zz}(i\omega_m)=-\int_0^\beta d\tau\, e^{i\omega_m\tau}\langle T_\tau\tilde{S}_{iz}(\tau)\tilde{S}_{jz}(0)\rangle\ , \tag{16}$$

where $\omega_m=2m\pi T$ are the Matsubara frequencies, $\beta=1/T$, $\mathbf{R}_i$ are the lattice vectors with $\mathbf{R}_1=0$, $T_\tau$ is the time-ordering operator, and the Heisenberg operator $A(\tau)$ is defined by

$$A(\tau)=e^{\tau H}Ae^{-\tau H}\ . \tag{17}$$

The transverse and longitudinal mode frequencies are given by the poles of the correlation functions $D_{+-}(\mathbf{k},\omega)$ and $D_{zz}(\mathbf{k},\omega)$, which are obtained from $D_{+-}(\mathbf{k},i\omega_m)$ and $D_{zz}(\mathbf{k},i\omega_m)$ by the analytic continuation $i\omega_m\rightarrow\omega+i\delta$.

In MF theory, with $H_2$ set to zero, these correlation functions are simple to evaluate. The correlation functions are then short ranged with

$$D_{ij}^{+-}(i\omega_m)=\delta_{ij}D_{+-}^{(0)}(i\omega_m)\ , \tag{18}$$

$$D_{+-}^{(0)}(i\omega_m)=\frac{2M_0}{\upsilon_0}\ , \tag{19}$$

$$D_{ij}^{zz}(i\omega_m)=\delta_{ij}D_{zz}^{(0)}(i\omega_m)\ , \tag{20}$$

$$D_{zz}^{(0)}(i\omega_m)=-\beta\delta_{m=0}G_1\ , \tag{21}$$

where $\Delta_0=zJM_0$, $\upsilon_0=i\omega_m-\Delta_0$, and the functions $G_n$ are defined by

$$G_n(T^*)=\langle S_{1z}^{n+1}\rangle_{\rm MF}=\frac{1}{Z_{00}}\sum_{m=-s}^{s}m^{n+1}e^{\beta^*mM_0}\ , \tag{22}$$

$$Z_{00}=\sum_{m=-s}^{s} e^{\beta^* m M_0} . \tag{23}$$

The zeroth-order function $G_0$ is equivalent to the MF order parameter. Both $zJD^{(0)}_{+-}(i\omega_m)$ and $zJD^{(0)}_{zz}(i\omega_m)$ are dimensionless functions of order $1/z^0$. Using Eqs. (18)–(21), we find that the Fourier-transformed correlation functions $D_{+-}(\mathbf{k},i\omega_m)$ and $D_{zz}(\mathbf{k},i\omega_m)$ are given by $D^{(0)}_{+-}(i\omega_m)$ and $D^{(0)}_{zz}(i\omega_m)$, independent of $\mathbf{k}$.

Analytically continued to real frequencies with $i\omega_m \rightarrow \omega + i\delta$, the MF transverse correlation function has a pole at the frequency $\Delta_0$. This pole corresponds to a single spin precessing about the local mean field $zJM_0$. A local precession of the spin involves both longitudinal and transverse fluctuations. While the transverse spin rotates about the $z$ axis with frequency $\Delta_0$, the longitudinal spin fluctuates from $s$ to $s-1$. At zero temperature, the cost in energy for this longitudinal fluctuation is $zJs$. At finite temperature, the energy cost is reduced to $zJM_0$.

Due to the coupling of spin fluctuations on neighboring sites, the spin excitations become collective and the pole at $\Delta_0$ is shifted to the SW frequency $\omega_{\mathbf{k}}$. Because of their collective nature, spin waves involve very small fluctuations of the longitudinal spin. When $\mathbf{k}\rightarrow\mathbf{0}$, the spin wave reduces to a small rotation of the total magnetization of the lattice and $\omega_{\mathbf{k}}$ tends to zero. However, we shall discover that spin waves with energies close to $\Delta_0$ couple to longitudinal fluctuations of the magnetization and to the propagating, precessional mode of the spin.

While the MF transverse correlation function depends on frequency, the MF longitudinal correlation function is static. As discussed in Sec. VI, the longitudinal fluctuations become dynamic when they couple to the transverse fluctuations Because of this difference between the MF correlation functions, we use slightly different methods to study the $1/z$ corrections to the transverse and longitudinal mode frequencies. The method described below is suitable only for the transverse correlation function. The method used to calculate the longitudinal mode frequencies is described in Sec. VI.

The exact, transverse correlation function can be expressed as

$$D_{+-}(\mathbf{k},i\omega_m)=\frac{D^{(0)}_{+-}(i\omega_m)}{1-D^{(0)}_{+-}(i\omega_m)\Sigma(\mathbf{k},i\omega_m)} , \tag{24}$$

where the self-energy $\Sigma(\mathbf{k},i\omega_m)$ is produced by the correlation of fluctuations on neighboring sites. This relation can inverted to yield the *definition* of the self-energy:

$$\Sigma(\mathbf{k},i\omega_m)=\frac{1}{D^{(0)}_{+-}(i\omega_m)}-\frac{1}{D_{+-}(\mathbf{k},i\omega_m)} . \tag{25}$$

Alternatively, Eq. (24) can be rewritten in terms of the real-space matrices $D^{+-}_{ij}(i\omega_m)$ and $\Sigma_{ij}(i\omega_m)$ as

$$\underline{D}(i\omega_m)=D^{(0)}_{+-}(i\omega_m)\underline{I}+D^{(0)}_{+-}(i\omega_m)\underline{\Sigma}(i\omega_m)\underline{D}(i\omega_m) , \tag{26}$$

where $\underline{I}$ is the identity matrix and $\Sigma(\mathbf{k},i\omega_m)$ is related to the self-energy matrix by

$$\Sigma(\mathbf{k},i\omega_m)=\sum_i e^{-i\mathbf{k}\cdot\mathbf{R}_i}\Sigma_{1i}(i\omega_m) . \tag{27}$$

Because $D^{(0)}_{+-}(i\omega_m)$ is nonzero for all $\mathbf{k}$ and all $m$, Eq. (24) and Eq. (26) provide equally general expressions for the correlation function. These equations make no other assumptions about the transverse correlation function or self-energy. A self-energy cannot be defined for the longitudinal correlation function because $D^{(0)}_{zz}(i\omega_m)$ vanishes when $m\neq 0$.

Because the mode frequencies are given by the zeroes of $[D_{+-}(\mathbf{k},\omega)]^{-1}$, the inverse correlation function or self-energy is really the object of interest. Strictly speaking, it is not necessary to construct a self-energy $\Sigma(\mathbf{k},i\omega_m)$ in order to expand $D_{+-}(\mathbf{k},i\omega_m)^{-1}$. The correlation function $D_{+-}(\mathbf{k},i\omega_m)$ may be expanded directly in powers of $1/z$, then inverted to obtain the mode frequencies, without ever defining a self-energy. However, certain simplifications occur when Eq. (26) is used to evaluate the self-energy. So, to calculate the transverse mode frequencies, we expand the self-energy; but to calculate the longitudinal mode frequencies, we must expand the correlation function directly.

Several steps are required to expand the self-energy $\Sigma(\mathbf{k},i\omega_m)$ in powers of $1/z$. First, every correlation function $D^{+-}_{ij}(i\omega_m)$ is expanded in powers of $1/z$. Then, Eq. (26) is inverted to obtain the $1/z$ expansion of the real-space self-energy $\Sigma_{ij}$. Finally, the Fourier transform in Eq. (27) yields the $1/z$ expansion of $\Sigma(\mathbf{k},i\omega_m)$, which can be written

$$\frac{\Sigma(\mathbf{k},i\omega_m)}{zJ}=\sigma_0(i\omega_m)+\frac{1}{z}\sigma_1(i\omega_m)+\cdots . \tag{28}$$

The self-energy is divided by $zJ$ so that the coefficients $\sigma_n$ are dimensionless functions of $T^*$, $i\omega_m/zJ$, the spin $s$, and the functions

$$\gamma^{(n)}_{\mathbf{k}}=\frac{1}{\mathcal{N}_n}\sum_{\delta^{(n)}} e^{i\mathbf{k}\cdot\delta^{(n)}} , \tag{29}$$

where the sum runs over the $\mathcal{N}_n$ different $n$-nearest-neighbor vectors $\delta^{(n)}$.

For a cubic lattice with the lattice constant set to 1, the first-order function is given by

$$\gamma^{(1)}_{\mathbf{k}}=\tfrac{1}{3}\{\cos(k_x)+\cos(k_y)+\cos(k_z)\} , \tag{30}$$

which equals 1 when $\mathbf{k}=\mathbf{0}$ and equals $-1$ when $\mathbf{k}=(\pm\pi,\pm\pi,\pm\pi)$. In an arbitrary lattice, $\gamma^{(1)}_{\mathbf{k}}=1$ when $\mathbf{k}=\mathbf{0}$ but $\gamma^{(1)}_{\mathbf{k}}$ does not always reach a minimum value of $-1$. Because $\gamma^{(1)}_{\mathbf{k}}$ sums over $\mathcal{N}_1=z$ different sites, $\gamma^{(1)}_{\mathbf{k}}$ is of order 1 in the $1/z$ expansion. For $n>1$, there is no simple relation between $\mathcal{N}_n$ and $z$ or between $\gamma^{(n)}_{\mathbf{k}}$ and $\gamma^{(1)}_{\mathbf{k}}$. Both $\mathcal{N}_{n>1}$ and $\gamma^{(n>1)}_{\mathbf{k}}$ can be expanded in powers of $1/z$. To lowest order in $1/z$, $\mathcal{N}_n=z^n/n!$ and $\gamma^{(n)}_{\mathbf{k}}=(\gamma^{(1)}_{\mathbf{k}})^n$.

Unlike the MF term $A_0$ in the expansion of $\langle A\rangle$, the zeroth-order term $\sigma_0(i\omega_m)$ in the expansion of $\Sigma(\mathbf{k},i\omega_m)$ is *not* the MF self-energy. As indicated by Eq. (25), $\sigma_0$ vanishes in MF theory and is nonzero due to the coupling of spin fluctuations on neighboring lattice sites. To cal-

culate $\sigma_0(i\omega_m)$, we must expand $D_{1j}^{+-}(i\omega_m)$ to order $1/z^n$, where $\mathbf{R}_j$ is the $n$th-nearest neighbor of $\mathbf{R}_1$. Then, Eq. (26) is inverted to obtain $\Sigma_{1j}(i\omega_m)$ to the same order. Finally, the Fourier transformation of Eq. (27) sums over the $z^n/n!$ equivalent lattice sites oriented around $\mathbf{R}_1$ to yield the zeroth-order self-energy $\sigma_0(i\omega_m)$. To evaluate $\sigma_1(i\omega_m)$, we must expand $D_{1j}^{+-}(i\omega_m)$ to order $1/z^{n+1}$, invert Eq. (26) to extract the self-energy, and Fourier transform to obtain the final result.

If the correlation function is evaluated among the $n$th-nearest neighbors of site 1, then the matrix elements $D_{1j}^{+-}(i\omega_m)$ are not all equal. For example, the next-nearest neighbors of $\mathbf{R}_1=\mathbf{0}$ can be divided into two classes: $\mathbf{R}_j=\pm\hat{\mathbf{x}}\pm\hat{\mathbf{y}}$ and $\mathbf{R}_{j'}=\pm 2\hat{\mathbf{x}}$ or $\pm 2\hat{\mathbf{y}}$. In the first class, $\mathbf{R}_j$ is a linear combination of different nearest-neighbor vectors $\boldsymbol{\delta}^{(1)}$; in the second class, $\mathbf{R}_{j'}$ cannot be expressed as such a linear combination. While the correlation functions are the same for $\mathbf{R}_j$ within either subclass, $D_{1j}^{+-}\neq D_{1j'}^{+-}$. In the evaluation of $\sigma_0$ or $\sigma_1$, only $D_{1j}^{+-}$ contributes: $D_{1j'}$ contributes to $\sigma_2$ but not to $\sigma_1$ or $\sigma_0$. More generally, among the $n$th-nearest neighbors of $\mathbf{R}_1$, we may restrict consideration to lattice sites $\mathbf{R}_j$ which are linear combinations of $n$ different nearest-neighbor vectors $\boldsymbol{\delta}^{(1)}$. Because $D_{1j}^{+-}$ and $\Sigma_{1j}^{+-}$ are the same for every $n$th-nearest neighbor in this subclass, we define $D_n(i\omega_m)$ to be the correlation function $D_{1j}^{+-}(i\omega_m)$ and $\Sigma_n(i\omega_m)$ to be the self-energy $\Sigma_{1j}(i\omega_m)$. These new quantities should not be confused with the coefficients in a $1/z$ expansion of the correlation function or self-energy.

## III. TRANSVERSE CORRELATION FUNCTION

To evaluate the $1/z$ corrections to the correlation function $D_n(i\omega_m)$, we expand Eq. (14) in powers of $\beta H_2$ and collect all the terms of a given order in $1/z$. To lowest order in this expansion, $D_n(i\omega_m)$ is of order $1/z^n$. The $1/z^n$ contribution to $D_n(i\omega_m)$ is represented by Fig. 1(a). A solid line represents a factor of $JR_{ij}$ coupling neighboring sites $i$ and $j$. Because $\mathbf{R}_j$ is the linear combination of $n$ different vectors $\boldsymbol{\delta}^{(1)}$, each of the $n$ lines coupling $\mathbf{R}_1$ to $\mathbf{R}_j$ must be oriented in a different direction. Hence, $D_n^{(a)}(i\omega_m)$ is proportional to $J^n=(zJ)^n/z^n$.

After a straightforward calculation, we find that the contribution of this "backbone" diagram is

$$D_n^{(a)}(i\omega_m)=(-1)^n\frac{2(zJ)^n n!}{z^n v_0^{n+1}}M_0^{n+1}\ , \tag{31}$$

where $v_0=i\omega_m-\Delta_0$ was defined earlier. Notice that $zJD_n^{(a)}(i\omega_m)$ is a dimensionless function of $i\omega_m/zJ$ and $M_0$. As expected, this function is of order $1/z^n$. For $n=0$, Eq. (31) reduces to the MF result of Eq. (19).

Inverting Eq. (26), we now solve for the self-energy matrix elements $\Sigma_n(i\omega_m)$. To order $1/z^n$, $\Sigma_1(i\omega_m)=-zJ/2z$ is the only nonzero matrix element. Hence, the zeroth-order term in the $1/z$ expansion of $\Sigma(\mathbf{k},i\omega_m)$ is given by

$$\sigma_0(i\omega_m)=-\tfrac{1}{2}\gamma_{\mathbf{k}}^{(1)}\ . \tag{32}$$

To this order in the expansion of the self-energy, the correlation function is

$$D_{+-}(\mathbf{k},i\omega_m)=\frac{2M_0}{i\omega_m-\Delta_0(1-\gamma_{\mathbf{k}}^{(1)})}\ . \tag{33}$$

Analytically continued to real frequencies, the correlation function has poles at the SW frequencies of the random-phase approximation[1]

$$\omega_{\mathbf{k}}=\Delta_0(1-\gamma_{\mathbf{k}}^{(1)})\ , \tag{34}$$

which vanishes when $\mathbf{k}=\mathbf{0}$. Thus, the pole in the MF correlation function at $\Delta_0$ is shifted by the coupling of transverse fluctuations to $\Delta_0(1-\gamma_{\mathbf{k}}^{(1)})$.

To evaluate the $1/z$ corrections to $\omega_{\mathbf{k}}$, we must calculate the $1/z^{n+1}$ corrections to $D_n(i\omega_m)$. These corrections are represented by Figs. 1(b)–1(f). Each of these diagrams modifies the backbone diagram in Fig. 1(a). In Fig. 1(b), a loop connects any site on the backbone to the $z-2$ sites around it. Since the contribution of the loop is proportional to $zJ^2=(zJ)^2/z$, it lowers the order of the diagram from $1/z^n$ to $1/z^{n+1}$. In Fig. 1(c), the loop is disconnected from the backbone. Because the loop can occupy $Nz/2$ positions in the lattice, $D_n^{(c)}(i\omega_m)$ includes extensive terms from both the numerator and denominator of the expectation value in Eq. (14). The extensive terms from the numerator and denominator cancel, leaving a finite contribution of order $1/z^{n+1}$. As shown in Fig. 1(d), lines in the $\pm\boldsymbol{\delta}$ directions may be inserted at any two points of the backbone. Since $\boldsymbol{\delta}$ can lie in $z-n$ different directions, the contribution of these inserted lines is proportional to $zJ^2=(zJ)^2/z$. So $D_n^{(d)}(i\omega_m)$ is of order $1/z^{n+1}$. Replacing any line of the backbone by a loop generates Fig. 1(e), which is also smaller by a factor of $J=(zJ)/z$ compared to the backbone diagram.

The final class of diagrams is shown in Fig. 1(f). In this diagram, a tadpole consisting of $m\geq 1$ lines terminating in a loop can be attached to any point on the diagram. Tadpole diagrams previously appeared in FL, where they renormalized the order parameter from $M_0$ to $M=M_0+M_1/z$. In this calculation, the tadpole diagrams replace $M_0$ by the shifted order parameter $M$ in Eq. (33) for $D_{+-}(\mathbf{k},i\omega_m)$ and in Eq. (34) for $\omega_{\mathbf{k}}$.

Because the full spin commutation relations are retained, Wick's theorem cannot be used to calculate the

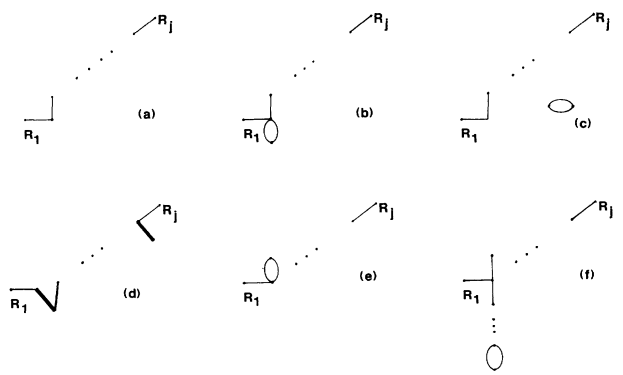


FIG. 1. The diagrams which contribute to the correlation function $D_n$.

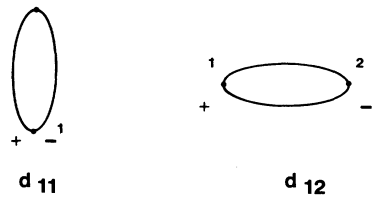


FIG. 2. Using the theorem proved in the Appendix, all other diagrams can be expressed in terms of these two basic diagrams.

contribution of these diagrams. A direct calculation of the correlation function is simplified by the theorem proved in the Appendix. Consider the contribution $A_{ij}^{(m)}(i\omega_n)$ of a diagram with $m$ lines coupling $\mathbf{R}_i$ with $\mathbf{R}_j$ in an arbitrary fashion. If another line is inserted between $\mathbf{R}_j$ and $\mathbf{R}_k$, then the contribution $A_{ik}^{(m+1)}(i\omega_n)$ is

$$A_{ik}^{(m+1)}(i\omega_n)=-\frac{zJM_0}{v_0}A_{ij}^{(m)}(i\omega_n)\ . \tag{35}$$

So, adding a line to one of the end points of a diagram simply multiplies that diagram's contribution by $-zJM_0/v_0$.

Therefore, the $1/z^{n+1}$ diagrams in Figs. 1(b)–1(f) can be simply evaluated in terms of the core diagram and the two building-blocks $d_{11}$ and $d_{12}$, shown in Fig. 2. Both of these basic diagrams can be evaluated without too much difficulty. Because $d_{11}$ can be oriented in $z$ different ways, its contribution is of order $zJ^2=(zJ)^2/z$. Diagram $d_{12}$, on the other hand, is of order $J^2=(zJ)^2/z^2$.

After cancelling the extensive terms which arise when the loop is disconnected from site 1, we find that

$$\begin{aligned}d_{11}(\tau)=&-\tfrac{1}{2}zJ^2(\tau-\beta)^2e^{-\Delta_0\tau}\langle R_{12}^2S_1^+S_1^-\rangle_{\mathrm{MF}}\\&-\tfrac{1}{2}zJ^2\tau^2e^{-\Delta_0\tau}\langle S_1^+R_{12}^2S_1^-\rangle_{\mathrm{MF}}\\&+zJ^2\tau(\tau-\beta)e^{-\Delta_0\tau}\langle R_{12}S_1^+R_{12}S_1^-\rangle_{\mathrm{MF}}\\&+\tfrac{1}{2}zJ^2\beta^2e^{-\Delta_0\tau}\langle S_1^+S_1^-\rangle_{\mathrm{MF}}\langle R_{12}^2\rangle_{\mathrm{MF}}\ .\end{aligned} \tag{36}$$

Notice that the time ordering automatically symmetrizes the $R_{12}$ and spin operators. Integrating over $\tau$ with Eq. (14), we find that

$$\begin{aligned}d_{11}(i\omega_m)=&\int_0^\beta d\tau e^{i\omega_m\tau}d_{11}(\tau)\\=&\frac{\beta^{*2}}{zv_0}\langle R_{12}^2\tilde{S}_{1z}\rangle_{\mathrm{MF}}+\frac{2zJ}{zv_0^2}f_2(T^*)\\&+2\frac{(zJ)^2}{zv_0^3}\langle S_{1z}\rangle_{\mathrm{MF}}\{\langle S_{1z}\rangle_{\mathrm{MF}}^2+f_1(T^*)\}\ ,\end{aligned} \tag{37}$$

where the dimensionless functions $f_1$ and $f_2$ are defined by

$$f_1(T^*)=2\langle\tilde{S}_{1z}^2\rangle_{\mathrm{MF}}\ , \tag{38}$$

$$f_2(T^*)=\frac{\beta^*}{4}\{4\langle\tilde{S}_{1z}^2\rangle_{\mathrm{MF}}+\langle S_1^+S_1^-\rangle_{\mathrm{MF}}\langle S_1^-S_1^+\rangle_{\mathrm{MF}}\}\ . \tag{39}$$

As expected, $zJd_{11}(i\omega_n)$ is a dimensionless function of order $1/z$.

We can similarly evaluate the contribution of $d_{12}$:

$$\begin{aligned}d_{12}(\tau)=&-\tfrac{1}{2}J^2(\tau-\beta)^2e^{-\Delta_0\tau}\langle R_{12}^2S_1^+S_2^-\rangle_{\mathrm{MF}}\\&-\tfrac{1}{2}zJ^2\tau^2e^{-\Delta_0\tau}\langle S_1^+R_{12}^2S_2^-\rangle_{\mathrm{MF}}\\&+zJ^2\tau(\tau-\beta)e^{-\Delta_0\tau}\langle R_{12}S_1^+R_{12}S_2^-\rangle_{\mathrm{MF}}\ .\end{aligned} \tag{40}$$

Integrating over $\tau$, we find

$$\begin{aligned}d_{12}(i\omega_m)=&\int_0^\beta d\tau e^{i\omega_m\tau}d_{12}(\tau)\\=&-\frac{2zJ}{z^2v_0^2}f_2(T^*)-2\frac{(zJ)^2}{z^2v_0^3}\langle S_{1z}\rangle_{\mathrm{MF}}f_1(T^*)\ ,\end{aligned} \tag{41}$$

which, aside from a couple of missing terms, is identical to $-d_{11}(i\omega_m)$.

Both $f_1$ and $f_2$ are easy to evaluate in terms of the $G_n$ function defined in Eq. (22). Each function is positive and vanishes like $e^{-s/T^*}$ in the limit of small temperatures. As $T^*$ approaches the MF Curie temperature $T_0=s(s+1)/3$, both $f_1$ and $f_2$ approach the finite limit $2s(s+1)/3$.

Figures 1(b)–1(e) can now be evaluated by multiplying Eqs. (37) and (41) by the appropriate factors of $-zJM_0/v_0$. Adding the contributions of Figs. 1(a)–1(f), we arrive at the final result

$$\begin{aligned}D_n(i\omega_m)=&(-1)^n\frac{2n!(zJ)^n}{z^nv_0^{n+1}}\langle S_{1z}\rangle_{\mathrm{MF}}^{n+1}\\&+(-1)^n\frac{n!(zJ)^n}{z^{n+1}v_0^{n+1}}\langle S_{1z}\rangle_{\mathrm{MF}}^{n-1}\left[(n+1)\beta^{*2}\frac{1}{1-f_3(T^*)}\langle S_{1z}\rangle_{\mathrm{MF}}\langle\tilde{S}_{1z}R_{12}^2\rangle_{\mathrm{MF}}+2nf_2(T^*)\right]\\&+(-1)^n\frac{n!(zJ)^{n+1}}{z^{n+1}v_0^{n+2}}\langle S_{1z}\rangle_{\mathrm{MF}}^{n}\left[(n+1)\beta^{*2}\frac{1}{1-f_3(T^*)}\langle S_{1z}\rangle_{\mathrm{MF}}\langle\tilde{S}_{1z}R_{12}^2\rangle_{\mathrm{MF}}+2nf_1(T^*)+2(n+1)f_2(T^*)\right]\\&+(-1)^n\frac{(n+1)!(zJ)^{n+2}}{z^{n+1}v_0^{n+3}}\langle S_{1z}\rangle_{\mathrm{MF}}^{n+1}[2f_1(T^*)+(2+n)\langle S_{1z}\rangle_{\mathrm{MF}}^2]\ .\end{aligned} \tag{42}$$

The scaling function $f_3$ previously appeared in our calculation of the $1/z$ correction to the order parameter.[6] Defined by

$$f_3(T^*)=\beta^*\langle \tilde{S}^2_{1z}\rangle_{\rm MF}=\frac{\beta^*}{2}f_1(T^*)\ , \tag{43}$$

this function vanishes at $T^*=0$ and reaches a maximum value of 1 at $T_0$. The terms in Eq. (42) proportional to $1/(1-f_3)$ are produced by the tadpole digrams in Fig. 1(f).

Unlike the expressions in the preceding paper[7] for the correlation function of a paramagnet, Eq. (42) for $D_n(i\omega_m)$ is valid for any $n\geq 0$. Such a general expression for the correlation function is now possible because the time-ordering operation automatically symmetrizes the spin operators, even when $n=0$ or 1.

We now use Eq. (26) to calculate the self-energy matrix elements $\Sigma_n(i\omega_m)$. To order $1/z^{n+1}$, only $\Sigma_0(i\omega_m)$ and $\Sigma_1(i\omega_m)$ are nonzero:

$$\Sigma_0(i\omega_m)\langle S_{1z}\rangle^2_{\rm MF}=\frac{v_0}{4z}\beta^{*2}\frac{1}{1-f_3(T^*)}\langle R^2_{12}\tilde{S}_{1z}\rangle_{\rm MF}+\frac{(zJ)^2}{2zv_0}f_1(T^*)\langle S_{1z}\rangle_{\rm MF}$$
$$+\frac{zJ}{4z}\left[\beta^{*2}\frac{1}{1-f_3(T^*)}\langle S_{1z}\rangle_{\rm MF}\langle R^2_{12}\tilde{S}_{1z}\rangle_{\rm MF}+2f_2(T^*)\right]\ , \tag{44}$$

$$\Sigma_1(i\omega_m)\langle S_{1z}\rangle^2_{\rm MF}=-\frac{zJ}{2z}\langle S_{1z}\rangle^2_{\rm MF}-\frac{(zJ)^2}{2z^2v_0}f_1(T^*)\langle S_{1z}\rangle_{\rm MF}-\frac{zJ}{2z^2}f_2(T^*)\ . \tag{45}$$

Therefore, the $1/z$ correction to the self-energy $\Sigma(\mathbf{k},i\omega_m)$ is

$$\sigma_1(i\omega_m)=\frac{v_0}{4}\beta^{*2}\frac{1}{1-f_3(T^*)}\langle R^2_{12}\tilde{S}_{1z}\rangle_{\rm MF}\left[1+\frac{zJ}{v_0}\langle S_{1z}\rangle_{\rm MF}\right]+\frac{zJ}{2}\left[f_2(T^*)+\frac{zJ}{v_0}\langle S_{1z}\rangle_{\rm MF}f_1(T^*)\right](1-\gamma^{(1)}_{\mathbf{k}})\ . \tag{46}$$

Like Eq. (32) for $\sigma_0$, this result is formally exact.

Inserting the results for $\sigma_0$ and $\sigma_1$ into the definition of the correlation function in Eq. (24), we find that

$$D_{+-}(\mathbf{k},i\omega_m)=2M\left[i\omega_m-\Delta(1-\gamma^{(1)}_{\mathbf{k}})-\frac{(zJ)^2}{z}(1-\gamma^{(1)}_{\mathbf{k}})\left[\frac{1}{i\omega_m-\Delta}f_1(T^*)+\frac{1}{\Delta}f_2(T^*)\right]\right]^{-1}\ , \tag{47}$$

where $M$ is the corrected order parameter $M_0+M_1/z$. Up to order $1/z$, we may also replace $M_0$ by $M$ in $\sigma_1$.

Finally, we construct the correlation function $D_{+-}(\mathbf{k},\omega)$ by replacing $i\omega_m\rightarrow\omega+i\delta$ in Eq. (47). The transverse mode frequencies are given by the poles of this correlation function. Due to the $f_1$ term in $\sigma_1$, the correlation function can be written as $2M(\omega-\Delta)$ divided by a quadratic equation. The two roots of that quadratic equation must be solved to obtain the mode frequencies. One root of the quadratic equation is close to the RPA frequency of Eq. (34), but shifted by terms of order $1/z$. Much more unexpectedly, the second root of the quadratic equation is close to the frequency $\Delta$. Since the correlation function is proportional to $(\omega-\Delta)$, the residue of this second pole is of order $1/z$. In the limit $z\rightarrow\infty$, the second pole disappears and the RPA frequencies become exact. As $T^*\rightarrow 0$, $f_1$ becomes exponentially small and the pole at $\Delta$ again disappears. At a given temperature $T^*>0$, the residue of the pole at $\Delta$ is a maximum when $\gamma^{(1)}_{\mathbf{k}}=0$ and decreases as the magnitude of $\gamma^{(1)}_{\mathbf{k}}$ increases.

The transverse mode frequencies are plotted as functions of $\gamma^{(1)}_{\mathbf{k}}$ in the solid lines of Figs. 3 and 4. At low temperatures, both $f_1$ and $f_2$ are of order $e^{-s/T^*}$ and the mode frequencies are very close to the RPA frequency $\Delta(1-\gamma^{(1)}_{\mathbf{k}})$ and to $\Delta$. Of course, the residue of the pole at $\Delta$ is also very small in this limit. But as the temperature increases, the correction terms $f_1$ and $f_2$ also increase and the modes repel. As $T^*/s(s+1)$ increases from 0.075 to 0.150, the repulsion between the transverse branches becomes quite evident.

When $\gamma^{(1)}_{\mathbf{k}}=0$, the splitting between the two branches is given by

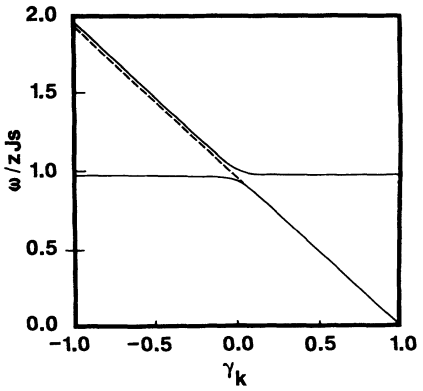


FIG. 3. The transverse mode frequencies $\omega/zJs$ vs $\gamma_{\mathbf{k}}$ for $z=12$, $s=\frac{7}{2}$, and $T^*/s(s+1)=0.075$. The dashed line is the Dyson-Maleev prediction.

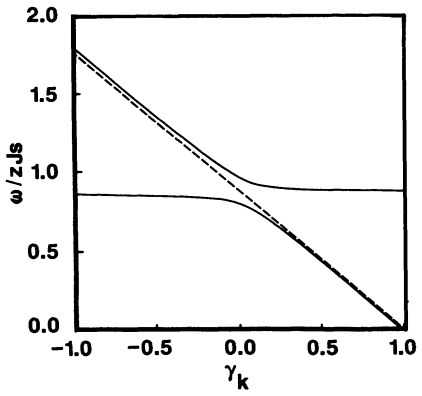


FIG. 4 Same as Fig. 3, except with $T^*/s(s+1)=0.15$.

$$\Delta\omega = 2zJ\sqrt{(1/z)f_1(T^*)}\ . \tag{48}$$

Because $\omega-\Delta$ enters the denominator of the $f_1$ term in the self-energy, the splitting $\Delta\omega/zJ$ is of order $1/z^{1/2}$ rather than of order $1/z$. Because $f_2$ produces a $1/z$ correction to $\Delta\omega/zJ$, we neglect its contribution in Eq. (48). As expected, the splitting between the branches tends to zero as $T^*\to 0$ or as $z\to\infty$, when MF theory becomes exact.

## IV. THE TRANSVERSE MODE FREQUENCIES

To understand the physics of this new transverse mode, we examine the origins of the $f_1$ term in the self-energy. This term, which is responsible for the new pole in the correlation function, appears in the basic diagrams $d_{11}$ and $d_{12}$. In $d_{12}$, $f_1$ arises from the antisymmetric combination of expectation values

$$\langle R_{12}^2 S_1^+ S_2^- \rangle_{\rm MF} + \langle S_1^+ R_{12}^2 S_2^- \rangle_{\rm MF} - 2\langle R_{12} S_1^+ R_{12} S_2^- \rangle_{\rm MF}\ , \tag{49}$$

which generates the $\tau^2$ contribution to $d_{12}(\tau)$ and the $1/v_0^3$ contribution to $d_{12}(i\omega_m)$. Each expectation value in Eq. (49) involves the product of a single longitudinal fluctuation and two transverse fluctuations on sites 1 and 2. In $d_{11}$, $f_1$ arises from the antisymmetric combination

$$-\langle R_{12}^2 S_1^+ S_1^- \rangle_{\rm MF} - \langle S_1^+ R_{12}^2 S_1^- \rangle_{\rm MF} + 2\langle R_{12} S_1^+ R_{12} S_1^- \rangle_{\rm MF}\ , \tag{50}$$

which generates the $\tau^2$ and $1/v_0^3$ contributions to $d_{11}(\tau)$ and $d_{11}(i\omega_m)$. Although the expectation values in Eq. (50) contain products that involve the transverse spin operators alone, the $f_1$ term appears only when the commutation relations between the longitudinal and transverse spin operators are scrupulously applied.

So, $f_1$ is produced by the coupling between the transverse and longitudinal fluctuations of the spin. At low temperatures, longitudinal fluctuations are suppressed and $f_1$ is exponentially small. But, at higher temperatures, longitudinal fluctuations are allowed and $f_1$ is non-negligible. As shown below, the coupling between the transverse and longitudinal fluctuations becomes significant above the crossover temperature $\bar{T}$.

Like $f_1$, the second correction term $f_2$ also contains contributions which couple the longitudinal and transverse fluctuations. But, unlike the $f_1$ contribution, the $f_2$ contribution to the self-energy neglects the dynamical effects of that coupling. In addition, $f_2$ also includes contributions which couple the transverse fluctuations to themselves.

At temperatures much lower than $\bar{T}$, both $f_1$ and $f_2$ are exponentially small and spin waves are the only transverse modes of the lattice. As the temperature increases, longitudinal fluctuations become more common and the propagation of the spin waves is disrupted. A longitudinal fluctuation on site $i$ forces the local spin to precess with the frequency $\Delta$ rather than with the SW frequency $\omega_{\mathbf{k}}$. Because the wave function of a spin wave contains a superposition of eigenstates, a spin wave with energy far from $\Delta$ can propagate through the longitudinal disturbance with a slight shift in energy. But when $\omega_{\mathbf{k}}$ is close to $\Delta$, the coupling between the spin waves and the longitudinal fluctuations induces a dramatic shift in the SW energy. This shift is evident in Figs. 3 and 4.

The precessional mode is excited by longitudinal fluctuations of the spin above $\bar{T}$. If a spin is decoupled from its neighbors, it precesses about the local mean field with frequency $\Delta$, independent of momentum. The pole in the MF correlation function at $\Delta$ is produced by such a local precession. Because the magnitude $\mathbf{S}_i\cdot\mathbf{S}_i = s(s+1)$ is constant, a longitudinal fluctuation on site $i$ coincides with the precession of $\mathbf{S}_i$ about the $z$ axis. Due to the coupling between $\mathbf{S}_i$ and the surrounding spins, the precessional mode can propagate through the lattice with a frequency which depends on momentum. In a hypercubic lattice, the dispersion of the precessional mode for small momentum is given by

$$\omega_{\mathbf{k}} \approx \Delta + \frac{zJ}{z^2}\frac{f_1(T^*)}{M}k^2\ . \tag{51}$$

As expected, this frequency tends to $\Delta$ as $T^*\to 0$ or as $z\to\infty$. Because the residue of the transverse pole is proportional to $(\omega-\Delta)$, the local precession of the spin cannot propagate through the lattice in the long-wavelength limit.

At the other edge of the Brillouin zone, when $\gamma_{\mathbf{k}}^{(1)}=-1$, the frequency of the precessional mode is given by

$$\omega_{\mathbf{k}} \approx \Delta - \frac{2zJ}{z}\frac{f_1(T^*)}{M}\ . \tag{52}$$

Because $(\omega-\Delta)$ is of order $1/z$, the precessional mode survives even when $\gamma_{\mathbf{k}}^{(1)}=-1$. Moreover, transverse modes cannot propagate with frequencies between $\Delta-2zJf_1/zM$ and $\Delta$. This small forbidden gap is created by the coupling between the transverse and longitudinal fluctuations.

In the long-wavelength limit $\gamma_{\mathbf{k}}^{(1)}=1$, the precessional mode cannot propagate and the SW modes are the only transverse excitations. But, for nonzero momentum, each branch of transverse excitations contains a mix be-

tween the SW and precessional modes. The mixing between the modes increases as $\gamma_{\mathbf{k}}^{(1)}$ decreases from 1, reaching a maximum at the mode-crossing point $\gamma_{\mathbf{k}}^{(1)}=0$. When $\gamma_{\mathbf{k}}^{(1)}>0$, the lower branch of the transverse modes is predominantly spin wave in nature; the upper branch is dominated by the propagating, precession of the spin. When $\gamma_{\mathbf{k}}^{(1)}<0$, the lower branch is dominated by the precessional mode and the upper branch is dominated by spin-waves.

To lowest order in $1/z$, only a pair of longitudinal fluctuations couple with the spin waves. As the order of the calculation increases, the number of possible longitudinal fluctuations grows. The likelihood of four longitudinal fluctuations disrupting the propagation of a spin wave is $1/z$ times smaller than the probability for a pair of such disturbances.

We emphasize that the precessional mode is a highly nonlinear fluctuation which only appears at high temperatures. While the spectral weight $A(\mathbf{k},\omega)$ now contains two peaks instead of one, the integral of $A(\mathbf{k},\omega)$ over frequency is not changed by the precessional mode. So the spectral weight of the transverse fluctuations is now shared among the SW and precessional modes of the lattice.

Because of the condition $\mathbf{S}_i\cdot\mathbf{S}_i=s(s+1)$, the longitudinal and transverse fluctuations of a ferromagnet are intimately related. This close relationship is embodied in the commutation relation between the various spin components. In the SW approximation, the spin operators are replaced with the Boson creation and annihilation operators $a_i$ and $a_i^\dagger$:

$$S_i^+\rightarrow\sqrt{2s}\,a_i\ , \tag{53a}$$

$$S_i^-\rightarrow\sqrt{2s}\,a_i^\dagger\ , \tag{53b}$$

$$\tilde{S}_{iz}\rightarrow\langle a_i^\dagger a_i\rangle-a_i^\dagger a_i\ , \tag{53c}$$

where $a_i$ and $a_i^\dagger$ obey the commutation relations

$$[a_i,a_j^\dagger]=\delta_{ij}\ . \tag{54}$$

With these replacements, the commutation relations between the spin operators are profoundly altered. For example, the commutator of $S_1^+$ and $S_1^-$ becomes $2s$ instead of $2S_{1z}$. Thus, the SW approximation grossly simplifies the dynamics of the longitudinal spin components.

If the spin operators in Eq. (49) or (50) are replaced by boson operators with the prescription of Eqs. (53a)–(53c), then Eq. (49) would vanish and the $f_1$ term would not appear in Eq. (50). Hence, the SW approximation ignores the precessional mode of the lattice. On the other hand, only the transverse contributions to $f_2$ survive when the spin operators are replaced by Boson operators. So the SW approximation does include the coupling between the transverse fluctuations.

In the Dyson-Maleev[2,9] (DM) version of the SW approximation, the SW frequencies are

$$\omega_{\mathbf{k}}^{\mathrm{DM}}=zJ\left\{s-\frac{1}{N}\sum_{\mathbf{q}}n_{\mathbf{q}}\right\}(1-\gamma_{\mathbf{k}}^{(1)})-\frac{zJ}{N}\sum_{\mathbf{q}}n_{\mathbf{q}}(\gamma_{\mathbf{q}-\mathbf{k}}^{(1)}-\gamma_{\mathbf{q}}^{(1)})\ . \tag{55}$$

The first momentum summation in Eq. (55) contains the change in the order parameter due to fluctuations. To order $1/z$ and at low temperatures, the order parameter $s-\sum_{\mathbf{q}}n_{\mathbf{q}}/N$ is equal to $M_0+M_1/z$. The second term in Eq. (55) is generated by the interactions among the spin waves. As expected, the DM theory ignores the coupling between the longitudinal fluctuations and the spin-waves.

To compare the DM theory with the $1/z$ expansion, we expand the SW frequencies of Eq. (55) in powers of $1/z$. The difference between the first-order, DM frequency $\omega_1^{\mathrm{DM}}$ and the exact, first-order frequency $\omega_1$ is plotted in Fig. 5 for $\gamma_{\mathbf{k}}^{(1)}=-1$. As shown, the deviation between $\omega_1^{\mathrm{DM}}$ and $\omega_1$ is exponentially small at low temperatures. But, as the temperature increases above a threshold, the difference between the two frequencies grows rather rapidly. In units of $T^*/s(s+1)$, this threshold temperature scales like $1/s$. Therefore, the DM theory becomes very accurate below a crossover temperature $\bar{T}$, which scales with the spin like $zJs$.

The arrows in Fig. 5 denote the crossover temperature $\bar{T}\approx 0.2zJs$ calculated previously in FV. In that paper, the free energy of the RPA approximation was compared with the exact free energy, up to order $1/z^2$. The deviation between the free energies becomes significant only above the crossover temperature $\bar{T}$. Below $\bar{T}$, the differences between the RPA and exact free energies are exponentially small and the SW approximation is accurate.

As seen in Fig. 5, the SW frequency of the DM theory deviates from the exact frequency above a crossover temperature very close to $\bar{T}$. Since this crossover is not sharp, we need not distinguish between the thermodynamic and dynamic crossover temperatures. One of the most important results of this paper is that the thermodynamic and dynamic crossovers coincide. In FV, Fishman and Vignale found that the thermodynamic crossover is marked by a peak in the fluctuation specific

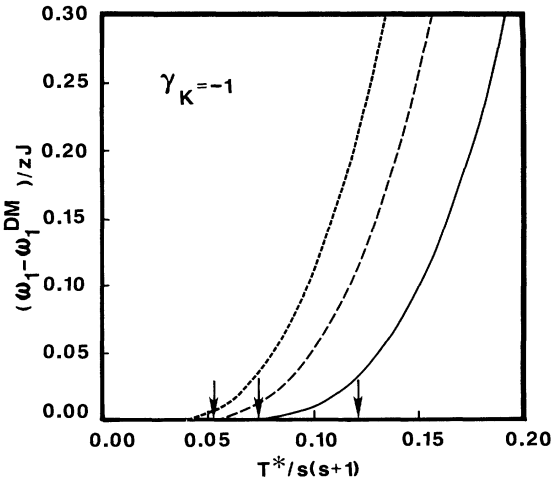


FIG. 5. The difference $(\omega_1-\omega_1^{\mathrm{DM}})/zJ$ between the exact $1/z$ frequency and the Dyson-Maleev result, evaluated to order $1/z$, vs $T^*/s(s+1)$. The differences plotted are for $s=\frac{1}{2}$ (solid), $s=\frac{3}{2}$ (dashed), and $s=\frac{5}{2}$ (small dash). The arrows denote the thermodynamic crossover temperature $\bar{T}^*=0.2/(s+1)$.

heat. Now we find that the dynamic crossover is marked by a much more spectacular effect: the splitting of the spin-wave resonance into two peaks.

At low temperatures, the difference between $\omega_{\mathbf{k}}^{\mathrm{DM}}$ and the SW $\omega_{\mathbf{k}}$ is

$$\omega_{\mathbf{k}}-\omega_{\mathbf{k}}^{\mathrm{DM}}=-\frac{2}{z}\frac{zJ}{s}y\frac{1-\gamma_{\mathbf{k}}^{(1)}}{\gamma_{\mathbf{k}}^{(1)}}+O(y^2)\ , \tag{56}$$

where $y=e^{-M/T^*}$. This difference is caused by the $f_1$ term in the self-energy, which is absent from the DM theory. Because the two branches of transverse excitations repel at $\gamma_{\mathbf{k}}^{(1)}=0$, Eq. (56) cannot be used near the mode crossing. Since $y$ is a function of $T^*/s$, Eq. (56) confirms that the crossover temperature $\bar{T}$ scales like $zJs$.

While the DM theory ignores the $f_1$ term in the self-energy, it does include the $f_2$ term. Expanded in order $1/z$ and evaluated at low temperatures, the second term in Eq. (55) agrees with the $f_2$ term in our theory. Therefore, this term does not contribute to the difference in Eq. (56). Notice that $f_2$ simply shifts the SW frequency while maintaining its proportionality to $(1-\gamma_{\mathbf{k}}^{(1)})$.

An obvious weakness of the self-energy expansion is its failure to yield the observed power-law corrections to the SW frequencies at low temperatures. These power-law corrections arise very naturally from the DM theory. For example, it can be shown[2] that, for small $k$ and $T$, $\omega_{\mathbf{k}}^{\mathrm{DM}}-sk^2/2z$ scales like $T^{5/2}$. Instead of power-law corrections, the $1/z$ expansion yields mode frequencies with exponential corrections of order $y\approx e^{-zJs/T}$.

As demonstrated in FV, the power-law corrections to thermodynamic quantities such as the free energy and specific heat can only be recovered by summing a selected group of exponential corrections to all orders in $1/z$. Such an unregulated summation is performed by the SW approximation and is justified below the crossover temperature $\bar{T}\propto zJs$. Similarly, in order to recover the power-law corrections to the SW frequencies at low temperatures, a selected group of self-energy terms must be summed to all orders in $1/z$. Such a summation is implicitly performed by the DM theory for the SW frequencies. Obviously, the $1/z$ results of Eq. (47) are not physically meaningful in this low-temperature regime. But the $1/z$ expansion is still mathematically rigorous at all temperatures. So the results of the $1/z$ expansion can be used to test the validity of the SW approximation. In this section, we have demonstrated that the unregulated $1/z$ summation of the SW approximation is only justified below the crossover temperature $\bar{T}$.

Since the DM frequency differs from the exact frequency by a term of order $y/z$, the unregulated summation of the SW approximation must be abandoned above the temperature $\bar{T}$, when $y$ becomes of order 1. Instead of $y$, $1/z$ becomes the relevant expansion parameter at high temperatures. So, above $\bar{T}$, the mode frequencies obtained from the correlation function of Eq. (47) become physically meaningful.

The $1/z$ expansion of the self-energy implicitly assumes that $\sigma_1$ is smaller than $\sigma_0$. This restriction can be written as $M_0^2/s^2\gg 1/z$. Using the MF expression for the order parameter near $T_C^*$, we find that the expansion of the self-energy to order $1/z$ is valid when

$$\frac{T_C^*-T^*}{T_C^*}\gg\frac{1}{z}\ . \tag{57}$$

Hence, the results of the previous section cannot be extrapolated arbitrarily close to $T_C^*$, where they would imply that the SW frequency $\omega_{\mathbf{k}}$ vanishes like $\Delta^3$ rather than like $\Delta$. As the order of the expansion increases, the range of validity of the expansion also grows. If the self-energy were expanded to order $1/z^2$, then Eq. (57) would be modified by replacing $1/z$ by $1/z^2$. But, even to order $1/z$, the range of temperatures satisfying Eq. (57) is quite large.

A self-energy expansion has also been used by Gros and Johnson[10] to study the dynamics of a spin-$\frac{1}{2}$ antiferromagnet at zero temperature. For $s=\frac{1}{2}$, the spin operators can be conveniently replaced by a set of fermion operators on each site. Wick's theorem can then be used to evaluate the correlation diagrams. Like the technique employed in this paper, the method of Gros and Johnson is a formally exact expansion of the self-energy in powers of $1/z$. Not surprisingly, they find that to lowest order in $1/z$, the RPA yields the correct mode frequencies of the antiferromagnet. Because they work at zero temperature, Gros *et al.* find that longitudinal fluctuations only renormalize the velocity of the SW mode.

## V. DAMPING OF THE TRANSVERSE MODES

Unfortunately, the self-energy expansion does not provide any information about the widths $\Gamma_1(\mathbf{k},\omega)$ and $\Gamma_2(\mathbf{k},\omega)$ of the SW and precessional modes. Since the imaginary part of Eq. (47) contains two $\delta$ functions, one at each pole, the widths $\Gamma_i$ of the modes must be nonanalytic functions of $1/z$ which vanish to any finite order in the $1/z$ expansion. This is confirmed by Vaks *et al.*,[8] who use a different technique to calculate the self-energy $\Sigma(\mathbf{k},i\omega_m)$. To order $1/z$, their result for $\Sigma(\mathbf{k},i\omega_m)$ agrees with ours. Moreover, their result for the width $\Gamma_1$ of the SW mode is a nonanalytic function of $1/z$.

Obviously, the momentum-space technique of Vaks *et al.*[8] is related to the $1/z$ expansion. Although Vaks *et al.* replace the spin operators by a set of fermion operators on every site, they preserve the original spin commutations by using Lagrange multipliers in the Hamiltonian. Rather than expand in powers of $1/z$, Vaks *et al.* expand the self-energy in powers of $1/r_0^3$, where $r_0$ is the range of the ferromagnetic coupling. When the coupling only extends to nearest neighbors, $r_0$ is equal to the lattice spacing.

An expansion in powers of $1/r_0$ is really an expansion in the number of momentum integrals. Since each momentum integral is proportional to $1/r_0^3$, the zeroth-order self-energy contains no momentum integrals and each contribution to the $1/r_0^3$ self-energy contains a single momentum integral. The real-space diagrams which con-

tribute to the $1/r_0^3$ correction are obtained from Figs. 1(b)–1(f) by replacing every loop with a sum over rings and by allowing each chain of lines to deform in any direction. As shown in FV, performing this procedure on the $1/z$ free energy yields the $1/r_0^3$ free energy calculated by Vaks *et al.* In the $1/r_0^3$ self-energy and free energy, every ring or chain diagram is allowed to intersect itself arbitrarily many times. Yet, each ring or chain diagram is evaluated as if only two lines couple at every point.[5] Clearly, this procedure is exact to order $1/z$. But, because the contributions of self-intersecting rings or chains are not subtracted to higher order in the $1/r_0^3$ expansion, this expansion cannot be exact to order $1/z^2$.

The $1/z$ expansion has many advantages over the $1/r_0^3$ expansion of Vaks *et al.* Unlike the $1/z$ expansion, the $1/r_0^3$ expansion lacks any formal expansion parameter. As previously demonstrated by Fishman and Vignale,[5] and $1/z$ expansion of the RPA free energy rapidly converges above the temperature $T_z \propto Js$. An examination of the first three terms in the $1/z$ expansion of the exact free energy suggests that the exact $1/z$ expansion also converges above $T_z$. So, above $T_z$, the $1/z$ expansion is probably convergent while the $1/r_0^3$ expansion has no formal justification. Another advantage of the $1/z$ expansion is that its consistency can be verified order by order. For instance, as shown in the previous paper,[7] the $1/z$ expansion of the Curie temperature for the ferromagnet and paramagnet are consistent.

On the other hand, the $1/r_0^3$ expansion yields the correct power-law corrections to the free energy, order parameter, and SW frequencies at low temperatures. As discussed above, the power-law corrections cannot be recovered by a finite expansion in powers of $1/z$. So, the method of Vaks *et al.* provides a useful interpolation between the low-temperature results of the SW approximation and an expansion to order $1/z$.

Because the $1/r_0^3$ expansion is exact to order $1/z$, the results of Vaks *et al.* provide a useful check on the results of the previous section. As mentioned above, our self-energy $\Sigma(\mathbf{k}, i\omega_m)$ agrees with the self-energy of Vaks *et al.*, evaluated to order $1/z$. Because their $1/r_0^3$ self-energy also contains terms of arbitrarily high order in a $1/z$ expansion, Vaks *et al.* failed to notice the second pole in the correlation function. Although their result for the width $\Gamma$ of the modes is not rigorous above the crossover temperature $\bar{T}$, it does provide a useful estimate for the lifetime of the excitations. Their expression for $\Gamma_1$ is given by

$$\frac{\Gamma_1^V(\mathbf{k},\omega)}{zJ} = \frac{\pi z J}{2N} f_1(T^*) \sum_{\mathbf{q}} \frac{(\gamma_{\mathbf{q}-\mathbf{k}} - \gamma_{\mathbf{q}})^2}{1-\gamma_{\mathbf{k}-\mathbf{q}} f_3(T^*)} \delta(\omega_{\mathbf{q}} - \omega) , \tag{58}$$

where $\omega_{\mathbf{q}}$ is the RPA frequency of Eq. (34). As expected, this expression vanishes to any finite order in $1/z$. Because $\Gamma_1^V$ is proportional to $f_1(T^*)$, the width of the SW mode becomes exponentially small as the temperature decreases.

As discussed by Vaks *et al.*, $\Gamma_1^V$ includes only the damping due to the coupling between the longitudinal and transverse fluctuations. It neglects the damping due to spin wave, spin-wave interactions, which dominate the attenuation below $\bar{T}$. Above $\bar{T}$, however, the damping due to the SW interactions may be neglected compared to the damping produced by longitudinal fluctuations.

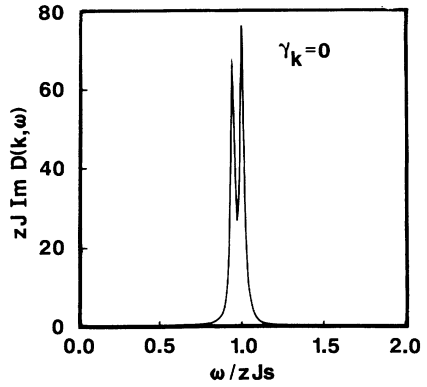


FIG. 6. The line shape of the transverse resonance for $z=12$, $s=\frac{7}{2}$, $T^*/s(s+1)=0.075$, $\Gamma=zJf_1/2$, and $\gamma_{\mathbf{k}}=0$.

Generally, the damping of the precessional and SW modes may be quite different. But at the mode crossing, the two modes are completely mixed and $\Gamma_1=\Gamma_2\equiv\Gamma$. So, to estimate the effect of damping on the observability of the precessional mode near the mode crossing, we simply replace $\omega$ by $\omega-i\Gamma$ in the correlation function. Using the result of Vaks *et al.* as a guide, we estimate $\Gamma\approx zJf_1/2$. The imaginary part of $D_{+-}(\mathbf{k},\omega)$ is plotted in Figs. 6–8 for $z=12$ and $s=\frac{7}{2}$. The two resonant peaks in Fig. 6 are plotted for $\gamma_{\mathbf{k}}^{(1)}=0$ and $T^*/s(s+1)=0.075$, which corresponds to a temperature of about $1.9\bar{T}$. If $\Gamma$ was 10 times larger, only a single peak would be observed at this temperature. With the same values for $\Gamma$ and $T^*$, but with $\gamma_{\mathbf{k}}^{(1)}=0.05$, the peak of the precessional mode is barely observable in Fig. 7. Hence, the splitting of the SW resonance may be observable only very close to the mode-crossing point $\gamma_{\mathbf{k}}^{(1)}=0$. As $\Gamma_2$ increases, the mode splitting becomes observable in a rapidly diminishing window of $\gamma_{\mathbf{k}}^{(1)}$. If the temperature is increased to $T^*/s(s+1)=0.15$, as in Fig. 8, then the splitting of the resonance peak may also be difficult to observe because of the large attenuation.

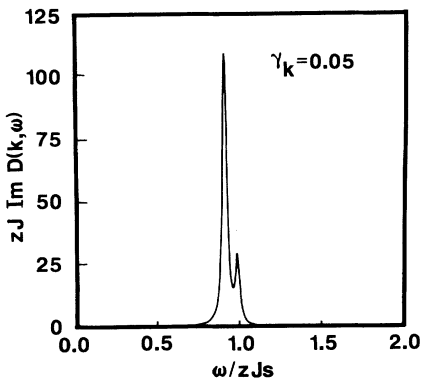


FIG. 7. Same as Fig. 6, except with $\gamma_{\mathbf{k}}=0.05$.

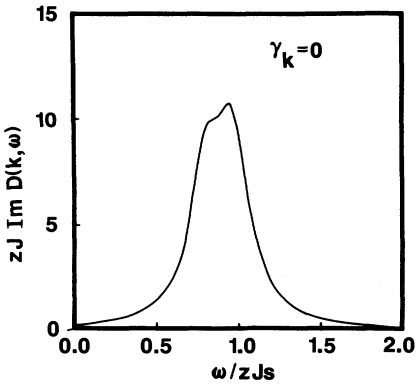


FIG. 8. Same as Fig. 6, except with $T^*/s(s+1)=0.15$.

Consequently, the splitting of the transverse resonance may be observable only in a narrow window of temperature and momentum. For the coupling term $f_1$ to be significant, the temperature must be above the crossover temperature $\bar{T}$. But, for too large a temperature, $\Gamma$ is of the same order as $\Delta$ and the splitting is not observable.

The splitting of the resonance is also more easily observed when the spin $s$ is small. Although $\bar{T}/T_C \propto 1/s$ increases as the spin decreases, longitudinal fluctuations couple more strongly to the transverse fluctuations for smaller spins. For example, with the same parameters used in Fig. 6 for $s=\frac{7}{2}$, the mode splitting $\Delta\omega/zJs$ increases by a factor of about 3 when $s=\frac{1}{2}$.

Under some conditions, the splitting of the resonance may be unobservable at any temperature. For example, if the precessional mode is overdamped so that $\Gamma_2-\Gamma_1 \gg \Delta$, then the SW mode will be relatively unaffected by the existence of the precessional mode, except in a very small region of energies around the mode-crossing point when $\Gamma_2 \approx \Gamma_1$. This appears to be the case[11] for EuO, which has a spin of $\frac{7}{2}$ and a face-centered-cubic structure.

Of course, if $\Gamma_2 \geq \Delta$, then both modes will be highly damped when $\gamma_{\mathbf{k}}^{(1)}=0$. So, even if a splitting of the transverse resonance is not observable, the damping of the spinwaves should become anomalously large at the mode-crossing point $\gamma_{\mathbf{k}}^{(1)}=0$. Unfortunately, this effect can be observed only in a very narrow window of momentum around $\gamma_{\mathbf{k}}^{(1)}=0$. As $\Gamma_2/\Delta$ increases, the size of this window rapidly decreases. In the absence of a mode splitting, it may also be possible to observe the systematic deviations of the SW frequencies from the DM predictions. But, as $\Gamma_2/\Delta$ increases, those deviations also become unobservable except very close to $\gamma_{\mathbf{k}}^{(1)}=0$.

## VI. LONGITUDINAL CORRELATION FUNCTION

As discussed above, the precession of a spin about the local mean field with frequency $\Delta$ coincides with the fluctuation of the longitudinal spin from $s$ to $s-1$. Hence, the precessional mode involves both longitudinal and transverse fluctuations of the spin. Yet this mode is fundamentally a transverse excitation which enters the transverse correlation function. To gain a better understanding of the longitudinal modes of a ferromagnet, we study the longitudinal correlation function directly.

Because the MF correlation function $D_{zz}^{(0)}(i\omega_m)$ vanishes when $m\neq 0$, a self-energy cannot be defined in terms of the longitudinal correlation function. But $D_{zz}(\mathbf{k},i\omega_m)$ may be expanded directly without employing a self-energy. The longitudinal mode frequencies are then given by the zeros of $[D_{zz}(\mathbf{k},\omega)]^{-1}$.

Such an approach was also possible for the transverse correlation function. However, the evaluation of the transverse mode frequencies was simpler with a self-energy. Because we used a self-energy, we could neglect matrix elements $D_{1j}^{+-}(i\omega_m)$ if $\mathbf{R}_j$ was not a linear combination of different nearest-neighbor vectors. If $D_{+-}(\mathbf{k},i\omega_m)$ was expanded directly, all matrix elements would contribute to the Fourier-transformed correlation function. Evaluating the self-energy matrix elements to order $1/z^n$, we discovered that only $\Sigma_0(i\omega_m)$ and $\Sigma_1(i\omega_m)$ were nonzero. Hence, the $1/z$ expansion of the self-energy only involved the function $\gamma_{\mathbf{k}}^{(1)}$ and not the higher-order functions $\gamma_{\mathbf{k}}^{(n>1)}$. A direct expansion of the correlation function would involve those higher-order functions and require that we expand $\gamma_{\mathbf{k}}^{(n)}$ in terms of $\gamma_{\mathbf{k}}^{(1)}$.

But a direct expansion of the longitudinal correlation function is actually very straightforward. Because it does not involve the transverse spin components, the MF longitudinal correlation function is static. The longitudinal dynamics are caused by the interactions between the longitudinal and transverse fluctuations. The diagrams that contribute to the longitudinal correlation function are the same as in Fig. 1, where operators $\tilde{S}_{1z}$ and $\tilde{S}_{jz}$ now occupy sites 1 and $j$. In this section, we evaluate the dynamic contributions to $D_{+-}(\mathbf{k},i\omega_m)$ which are nonzero when $\omega_m\neq 0$. Using a modified version of the proof in the Appendix, we have shown that the contribution of any diagram with a single line between neighboring sites must vanish for nonzero $\omega_m$. So, the only diagrams which contribute to the dynamics of the correlation function are identical to $d_{11}$ and $d_{12}$ of Fig. 2, except that the $S_i^{\pm}$ operators are replaced by $\tilde{S}_{iz}$ operators on sites 1 and 2.

Evaluating these diagrams, we find that

$$d_{11}(i\omega_m)=\frac{zJ}{z(i\omega_m)^2}f_4(T^*)\,, \tag{59}$$

$$d_{12}(i\omega_m)=-\frac{1}{z}d_{11}(i\omega_m)\,, \tag{60}$$

where

$$f_4(T^*)=\frac{\beta^*}{2}\langle S_1^- S_1^+\rangle_{\mathrm{MF}}\langle S_1^+ S_1^-\rangle_{\mathrm{MF}}\,. \tag{61}$$

So for $m\neq 0$, the longitudinal correlation function is

$$D_{zz}(\mathbf{k},i\omega_m)=\frac{zJ}{z(i\omega_m)^2}f_4(T^*)(1-\gamma_{\mathbf{k}}^{(1)})\,. \tag{62}$$

Analytically continued to real frequencies, the longitudinal correlation function has a second-order pole at zero frequency. The longitudinal correlation function was also calculated by Vaks *et al.*[8] Expanded to order $1/z$, their expression for $D_{zz}(\mathbf{k},i\omega_m)$ agrees with Eq. (62).

As discussed in the previous section for the transverse

correlation function, the expansion of the longitudinal correlation function to order $1/z$ is only valid for temperatures above $T_z$ and satisfying Eq. (57). Hence, Eq. (62) does not imply that the longitudinal pole at zero frequency persists even at the Curie temperature.

As $T^* \to 0$, $f_4$ becomes exponentially small and the dynamics induced by the transverse fluctuations disappears. But at finite temperature and for nonzero momentum the longitudinal correlation function diverges at zero frequency. Due to the coupling with the transverse fluctuations, the longitudinal mode has zero frequency: an arbitrarily small rotation of the spin from the $z$ axis requires no energy if the neighboring spins rotate in response.

Hence, we must carefully distinguish between the precessional mode and the longitudinal mode of the lattice. While the precessional mode involves the quantum fluctuation of the longitudinal spin from $s$ to $s-1$, the longitudinal mode involves the small rotations of the spin from the $z$ axis. Another major difference is that, unlike the precessional mode, the longitudinal mode does not propagate through the lattice. This is easily seen from the diagrams which contribute to the longitudinal and transverse correlation functions. The diagrams $d_{11}$ and $d_{12}$ which contribute to $D_{zz}(\mathbf{k}, i\omega_m)$ only couple neighboring lattice sites; the diagrams in Fig. 1 which contribute to $D_{+-}(\mathbf{k}, i\omega_m)$ span the whole lattice. So, a longitudinal fluctuation on site $i$ can only travel as far as its neighboring site, while a transverse fluctuation can tour the whole lattice.

Experimentally,[12,13] longitudinal fluctuations have been observed only very close to the Curie temperature. Using polarized neutron scattering, Mitchell, Cowley, and Pynn[12] and Boni, Martinez, and Tranquada[13] have measured the quasielastic peak due to longitudinal fluctuations centered around zero frequency. As expected from our discussion, the longitudinal fluctuations are diffusive and do not propagate through the lattice. The integrated intensity of the longitudinal peak decrease as the temperature is lowered and as the wave vector increases. Sufficiently far away from the Curie temperature, the longitudinal peak cannot be resolved. While the dynamical calculations of this paper cannot be applied in the region of the Curie temperature, they do confirm that longitudinal modes do not propagate above the crossover temperature $\bar{T}$.

## VII. CONCLUSION

The fundamental assumption of this work is that the $1/z$ expansion of the self-energy converges. If this expansion does converge, then the transverse correlation function must have two poles instead of one. The existence of the precessional mode has many consequences for the high-temperature properties of a ferromagnet. The most dramatic consequence awaits experimental confirmation: the splitting of the transverse resonance peak near $\Delta$. Another consequence may be more difficult to observe: a gap of order $1/z$ in the frequency spectrum of the transverse modes.

Away from the mode-crossing point, we have found small but significant shifts in the SW frequencies from the predictions of the SW approximation. Indeed, it is remarkable that the high-temperature, nonlinear excitations of a ferromagnet have frequencies so close to the RPA frequencies. The result of the RPA is incredibly robust. It survives as the lowest-order term in a high-temperature, $1/z$ expansion and as the lowest-order term in a low-temperature, SW approximation. Only the next-order corrections to the mode frequencies distinguish the nonlinear regime above $\bar{T}$ from the linear regime below it. Understandably, the accuracy of the RPA has inspired great confidence in the SW approximation. While that confidence is surely warranted below $\bar{T}$, it is almost certainly misplaced above that crossover temperature.

## ACKNOWLEDGMENTS

We would like to acknowledge support from the U.S. Department of Energy under Contract No. DE-AC05-84OR21400 with Martin Marietta Energy Systems, Inc., from the National Science Foundation under Grant No. DMR-8704210, and from the EPSCOR program in North Dakota. Useful conversations with Dr. M. Johnson, Dr. J. Fernandez-Baca, and especially with Dr. G. Vignale are also gratefully acknowledged.

## APPENDIX

This appendix proves Eq. (35), which allowed us to evaluate the diagrams in Fig. 1 in terms of the two basic diagrams $d_{11}$ and $d_{12}$ of Fig. 2. In Fig. 9(a), $A_{ij}^{(m)}$ is the contribution of a digram with $m$ lines joining sites $i$ and $j$ in some arbitrary fashion. Inserting a line between site $j$ and site $k$ leads to the second diagram, $A_{ik}^{(m+1)}$, with $m+1$ lines joining sites $i$ and $k$. Transverse spin operators act on the sites $i$, $j$, and $k$, as shown. In this appendix, we show that $A_{ik}^{(m+1)}(i\omega_n)$ is equal to $A_{ij}^{(m)}(i\omega_n)$ times the factor $-zJM_0/v_0$.

The contribution of $A_{ij}^{(m)}(\tau)$ is given by

$$A_{ij}^{(m)}(\tau) = -(-1)^m (zJ)^m \times \sum_{r=0}^{m} \begin{bmatrix} m \\ r \end{bmatrix} (\tau-\beta)^{m-r}(-\tau)^r e^{-\Delta\tau} F_{ij}^{(m,r)} , \tag{A1}$$

$$F_{ij}^{(m,r)} = \frac{1}{m!} \langle P(R \cdots RS_i^+ R \cdots RS_j^-) \rangle_{\mathrm{MF}} , \tag{A2}$$

where Eq. (A2) contains the product of $m-r$ different $R_{\alpha\gamma}$ operators before $S_i^+$ and $r$ different $R_{\alpha\gamma}$ operators

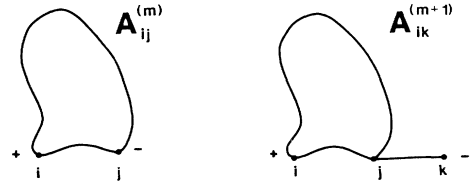


FIG. 9. $A_{ij}^{(m)}$ represents a diagram with $m$ lines coupling $S_i^+$ and $S_j^-$. $A_{ik}^{(m+1)}$ represents the same diagram with an additional line between $S_j^+$ and $S_k^-$.

after. The permutation operator in Eq. (A2) does not move the spin operators $S_i^+$ or $S_j^-$, but does sum over distinct permutations of the $m$ different $R_{\alpha\gamma}$ operators which join sites $i$ and $j$. Fourier transformed, $A_{ij}^{(m)}(i\omega_n)$ is given by

$$A_{ij}^{(m)}(i\omega_n)=\int_0^\beta d\tau\, e^{i\omega_n\tau}A_{ij}^{(m)}(\tau)\ . \tag{A3}$$

Similarly, $A_{ik}^{(m+1)}(\tau)$ is given by

$$A_{ik}^{(m+1)}(\tau)=-(-1)^{m+1}(zJ)^{m+1}\times\sum_{r=0}^{m+1}\begin{bmatrix}m+1\\ r\end{bmatrix}(\tau-\beta)^{m+1-r}(-\tau)^r\times e^{-\Delta\tau}F_{ik}^{(m+1,r)}\ , \tag{A4}$$

where $F_{ik}^{(m+1,r)}$ is obtained from Eq. (A2) by replacing $m$ by $m+1$.

Since $A_{ik}^{(m+1)}$ contains a single line coupling sites $j$ and $k$, we may replace $R_{jk}$ in $F_{ik}^{(m+1,r)}$ by $S_j^-S_k^+/2$. Hence, we find that

$$F_{ik}^{(m+1,r)}=\frac{1}{2(m+1)!}\langle S_k^+S_k^-\rangle_{\rm MF}\times\langle P(R\cdots RS_i^+R\cdots RS_j^-)\rangle_{\rm MF}\ , \tag{A5}$$

where now the first group contains $m+1-r$ operators and the second group $r-1$ of the $R_{\alpha\gamma}$ operators. In addition, the permutation operator now operates on $S_j^-$.

We now perform the permutation operation on $S_j^-$ in Eq. (A5). If $S_j^-$ moves among the $r$ positions to the right of $S_i^+$, then a rearrangement of the $R_{\alpha\gamma}$ operators yields a sum over $F_{ij}^{(ms)}$ from $s=0$ to $s=r-1$. If $S_j^-$ moves among the $m+1-r$ positions to the left of $S_i^+$, then rearranging the $R_{\alpha\gamma}$ and $S_j^-$ operators produces a sum over $F_{ij}^{(m,r+s)}e^{-\Delta\beta}$ from $s=0$ to $s=m-r$. So, after performing all possible permutations of the $S_j^-$ operator, we find

$$F_{ik}^{(m+1,r)}=\frac{1}{2(m+1)}\langle S_k^+S_k^-\rangle_{\rm MF}\times\left[\sum_{s=0}^{r-1}F_{ij}^{(m,s)}+e^{-\Delta\beta}\sum_{s=0}^{m-r}F_{ij}^{(m,r+s)}\right]\ . \tag{A6}$$

After Fourier transforming $A_{ik}^{(m+1)}(\tau)$ with Eq. (A3) and integrating by parts, we find

$$\begin{aligned}A_{ik}^{(m+1)}(i\omega_n)&=\frac{1}{2(m+1)}(-1)^m(zJ)^m\langle S_1^+S_1^-\rangle_{\rm MF}\frac{1}{v_0}\\&\times\int_0^\beta d\tau\, e^{i\omega_n\tau}e^{-\Delta\tau}\left[\sum_{r=0}^{m}(\tau-\beta)^{m-r}(-\tau)^r(m+1-r)-\sum_{r=1}^{m+1}r(\tau-\beta)^{m+1-r}(-\tau)^{r-1}\right]\\&\times\begin{bmatrix}m+1\\ r\end{bmatrix}\left[\sum_{s=0}^{r-1}F_{ij}^{(m,s)}+e^{-\Delta\beta}\sum_{s=0}^{m-r}F_{ij}^{(m,r+s)}\right]\\&=\tfrac{1}{2}(-1)^{m+1}(zJ)^{m+1}\langle S_1^+S_1^-\rangle_{\rm MF}\frac{1}{v_0}\int_0^\beta d\tau\, e^{i\omega_n\tau}e^{-\Delta\tau}\sum_{r=0}^{m}(\tau-\beta)^{m-r}(-\tau)^r\begin{bmatrix}m\\ r\end{bmatrix}(-F_{ij}^{(m,r)}+e^{-\Delta\beta}F_{ij}^{(m,r)})\\&=-\frac{zJM_0}{v_0}A_{ij}^{(m)}(i\omega_n)\ ,\end{aligned} \tag{A7}$$

where $v_0=i\omega_n-\Delta$. If a line were added to the other end point of $A_{ij}^{(m)}$, the same result would be found

*Permanent address.

[1]See, for example, R. M. White, *Quantum Theory of Magnetism* (Springer-Verlag, Berlin, 1963); or D. C. Mattis, *The Theory of Magnetism I* (Springer, Berlin, 1988), Chap. 5.

[2]F. J. Dyson, Phys. Rev. **102**, B1217 (1956); **102**, B1230 (1956).

[3]O. W. Dietrich, J. Als-Nielsen, and L. Passell, Phys. Rev. B **14**, 4923 (1976).

[4]H. G. Bohn, A. Kollmar, and W. Zinn, Phys. Rev. B **30**, 6504 (1984).

[5]R. S. Fishman and G. Vignale, Phys. Rev. B **44**, 658 (1991).

[6]R. S. Fishman and S. H. Liu, Phys. Rev. B **40**, 11 028 (1989).

[7]R. S. Fishman and S. H. Liu, preceding paper, Phys. Rev. B **45**, 5406 (1992).

[8]V. G. Vaks, A. I. Larkin, and S. A. Pikin, Zh. Eksp. Teor. Fiz. **53**, 281 (1967) [Sov. Phys. JETP **26**, 188 (1968)]; **53**, 1089 (1967) [**26**, 647 (1968)].

[9]S. V. Maleev, Zh. Eksp. Teor. Fiz. **34**, 1518 (1958) [Sov. Phys. JETP **7**, 1048 (1958)].

[10]Claudius Gros and M. D. Johnson, Phys. Rev. B **40**, 9423 (1989); M. D. Johnson, Claudius Gros, and K. J. von Szczepanski, *ibid.* **43**, 11 207 (1991).

[11]J. Fernandez-Baca and H. A. Mook (unpublished).

[12]P. W. Mitchell, R. A. Cowley, and R. Pynn, J. Phys. C **17**, L875 (1984).

[13]P. Boni, J. L. Martinez, and J. M. Tranquada, Phys. Rev. B **43**, 575 (1991).